Forced decadal changes in summer precipitation characteristics over China: the roles of greenhouse gases and anthropogenic aerosols

Article

Accepted Version

Zhang, B., Dong, B. ORCID: https://orcid.org/0000-0003-0809-7911 and Jin, R. (2021) Forced decadal changes in summer precipitation characteristics over China: the roles of greenhouse gases and anthropogenic aerosols. Journal of Meteorological Research, 34 (6). pp. 1226-1241. ISSN 2198-0934 doi: 10.1007/s13351-020-0060-4 Available at https://centaur.reading.ac.uk/91968/

To link to this article DOI: http://dx.doi.org/10.1007/s13351-020-0060-4

Publisher: Springer

Forced decadal changes in summer precipitation characteristics over China: the roles of greenhouse gases and anthropogenic aerosols

Zhang Bo[1*] Buwen Dong[2] Ronghua Jin[1]
[1] National Meteorological Center, Beijing, China
[2] National Center for Atmospheric Science-Climate, Department of Meteorology, University of Reading, Reading, UK

Abstract

We investigated the decadal changes in the different types of summer mean precipitation over China across the mid-1990s based on observational datasets. The spatial variations in the observed decadal changes were estimated by comparing the present day time period of 1994–2011 with an earlier period of 1964–1981. The summer total precipitation increased in southern China and decreased in northern China from the early period to the present day. The increases of precipitation in southern China were due to increases in the frequency of heavy and moderate rainfall, whereas the decreases over northern China were mainly due to decreases in the frequency of moderate and light rainfall. Based on a set of numerical experiments using an atmospheric general circulation model coupled with a multi-level mixed-layer ocean model, we found that the increase of precipitation frequency forced by greenhouses gases is the main reason of increasing precipitation over southern and northeastern China, while the decrease of frequency caused by anthropogenic aerosols induces the decreasing precipitation over northern China. The water vapor flux convergence and water vapor flux strengthens in southern China and northeastern China by anthropogenic greenhouses gases. This distribution is also conductive to precipitation in most of southern China and northeastern China. Under the control of weaken southwesterly winds and 850-

hPa divergence, precipitation decreases over northern and southwestern China by anthropogenic aerosols.

Keywords: decadal changes in precipitation; frequency and intensity; numerical experiments; China

1. Introduction

China is located in the Asian monsoon region and precipitation in summer is mainly controlled by the East Asian summer monsoon. A decadal shift occurred in East China in the late 1970s, with more precipitation in the Yangtze River valley and less precipitation in northern China (Wu and Chen 1998; Gong and Ho 2002; Yu et al.2004; Zhai et al. 2005; Ding et al. 2008; Qian and Qin 2008; Zhao et al. 2010). Summer precipitation over southern China then increased after 1992/1993(Yao et al. 2008; Ding et al. 2009; Wu et al. 2010; Fan et al. 2014; Xu et al. 2015).There have been many studies of the decadal variations in different types of precipitation (Qian and Qin 2008; Wang et al. 2011; Yang and Li 2014; He and Zhai 2018). Under the current conditions of global climate change, the amount of heavy precipitation in eastern China has increased (Wang et al. 2011; Yang and Li 2014) and the contribution of extreme precipitation to the total amount of precipitation in summer has also increased in most parts of China (Min and Qian 2008; He and Zhai 2018), although precipitation has decreased in central Inner Mongolia and the Sichuan Basin (He and Zhai 2018). The frequency and amount of light rainfall in eastern China have shown decreasing trends since the 1950s (Qian et al. 2009; Rajah et al. 2014).

Many researchers have investigated the possible causes of changes in precipitation in China (Yu et al. 2004; Yu and Zhou 2007; Zhou et al. 2009).The impact of human activity on changes in precipitation has been studied in some regions, including land at high latitudes in the northern hemisphere (Min and Qian 2008; Wan et al. 2015), South Asia (Bollasina et al. 2011) and East Asia (Ma et al. 2017b). Because variations of the East Asian summer monsoon and related rainfall can be caused by both changes in anthropogenic forcing and natural variability, many previous studies have analysed the relative importance of these variations (Shen et al. 2008; Wang et al. 2012,2013; Song et al. 2014). Some studies have shown that changes in greenhouse gas (GHG) concentrations and anthropogenic aerosol(AA) emissions are the most important factors for the Southern-Flood–Northern-Drought pattern (SFND) (Chen and Sun 2017; Ma et al. 2017b; Wang et al. 2013; Xie et al. 2016; Zhang et al. 2017; Dong et al. 2016;Tian et al. 2018). The amount of precipitation in southern China increases with an increase in GHG concentrations, whereas changes in anthropogenic aerosols dominate the drought conditions in northern China. Forcing by anthropogenic aerosols weakens the East Asian summer monsoon, which leads to divergent wind anomalies and reduced precipitation in northern China (Tian et al.2018). The decrease in light rainfall in recent decades is mainly due to dramatic increases in anthropogenic aerosols (Qian et al. 2009; Rosenfeld et al. 2007;Wang et al. 2016). A study by Liu et al. (2015) showed that global climate change rather than aerosol effects is the main reason for the change in the intensity of precipitation in eastern China.

A large number of global climate models have projected that climate extremes (such as extreme precipitation and the number of consecutive dry days and extremely hot days) will increase with increases in the concentrations of GHGs and decreases in aerosol emissions (Caesar and Lowe 2012; Kharin et al. 2013; Sillmann et al. 2013a; Zhou et al. 2014). The response of precipitation to global climate change takes two forms: an increase in the total amount of rainfall and an increase in the rain rates of the heaviest events. Trenberth (1999) explained that this differences meansthat the frequency of precipitation changes toward more heavy rains and a decrease of rainfall frequency. Based on Phase 5 of the Coupled Model Intercomparison Project (CMIP5), Pendergrass and Hartmann (2014a) found that rain rates are increasing with global climate change. Using CAM5 model experiments, Wang et al.(2016) found that dramatic increases in anthropogenic aerosols are the main reason for the observed decrease in light rainfall in eastern China since the 1950s.

Most published studies have focused on the decadal variations in extreme and light precipitation and how these are affected by human activity. By contrast, the variations indifferent magnitudes of precipitation, especially the changes in the frequency and intensity of rainfall in recent decades, are still unclear. The individual contributions of changes in GHG concentrations and emissions of anthropogenic aerosols to the recent decadal changes in precipitation have not yet been assessed. Therefore the main aims of this work were:(1) to investigate recent decadal changes in the characteristics of summer precipitation (light, moderate and heavy rainfall), their spatial variation and their contributions to the summer mean precipitation over China; and (2) to quantify the relative roles of changes in GHG concentrations and the emission of anthropogenic aerosols in shaping these changes.

The rest of this paper is organized as follows:Section 2 revisits the observed decadal changes ofthe mean summer precipitation and the characteristics of precipitation over China. Section 3 describes the model and experiments and Section 4 reports the simulated changes in response to different changes in anthropogenic forcing. Section 5 describe the initial physical processes of simulating precipitation changes through different anthropogenic forcings, such as GHG concentrations and AA emissions. Finally, a summary and discussion are summarized in Section 6.

2. Observed decadal changes in precipitation characteristics over China

2.1 Observational datasets

The daily rainfall data used in this study were selected from the daily rainfall datasets of 2474 stations in China from 1960 to 2013 provided by the National Meteorological Information Center, China Meteorological Administration (Ren et al. 2012).As a result of the construction and removal of individual stations during this time period, 1361 stations were finally included in this study (Fig.2a). The summer mean precipitation refers to the mean precipitation from June to August.

2.2 Definition

Because there are many different types of climate in China, the absolute precipitation threshold cannot be used to distinguish the type of precipitation. A percentile value was therefore used to determine the threshold of different types of precipitation. The two relative thresholds of three different types of precipitation on each calendar day for each station were calculated during the baseline period of 1964–1981.The first threshold was the 90th percentile and the second was the 60th percentile of precipitation.

Daily precipitation in China was divided into three types: (1) heavy precipitation (i.e., precipitation above the 90th percentile); (2) moderate precipitation (i.e., precipitation between the 90th and 60th percentiles); and (3) light precipitation (i.e., precipitation below the 60thpercentile).

Summer precipitation and its characteristics were studied based on the frequency, intensity and number of dry days. A dry day was defined as a day with daily precipitation <1 mm. The frequency was defined as the cumulative number of days in a certain category of precipitation in the summer of one year. The corresponding intensity was calculated from the average intensity of all events.

2.3 Observed decadal change

Figure 1a, 1c, 1e and 1g show the spatial distribution of the annual average summer precipitation and the contribution of heavy, moderate and light rainfall, respectively, to the observations during the period from 1994 to 2011.Influenced by the East Asian summer monsoon, summer precipitation in China is mainly concentrated in southeastern China, while the precipitation in northwestern China is less than that in southeastern China. Heavy rainfall accounts for about 40–50% of summer precipitation in eastern China and about 20–40% in western China (Fig. 1c). Moderate rainfall accounts for about 40–50% of summer precipitation (Fig. 1e), whereas the contribution of light rainfall is in the form of west more and east less and accounts for <20% of precipitation in eastern China and 20–30% in western China.

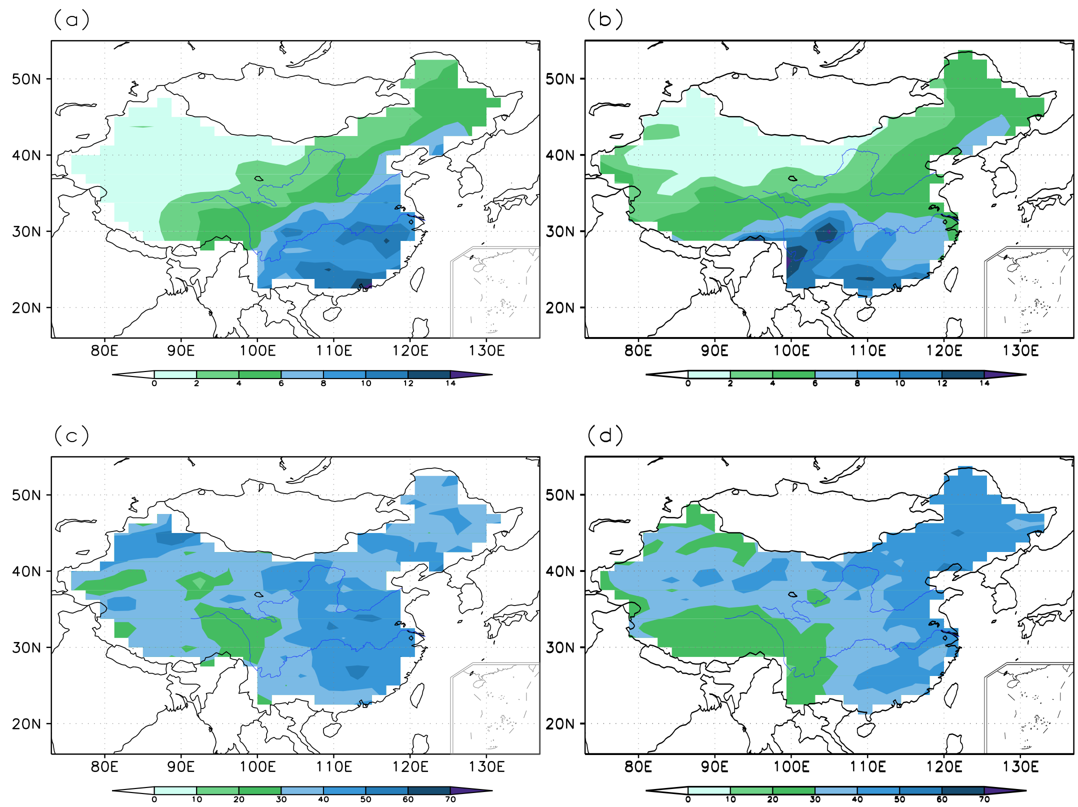

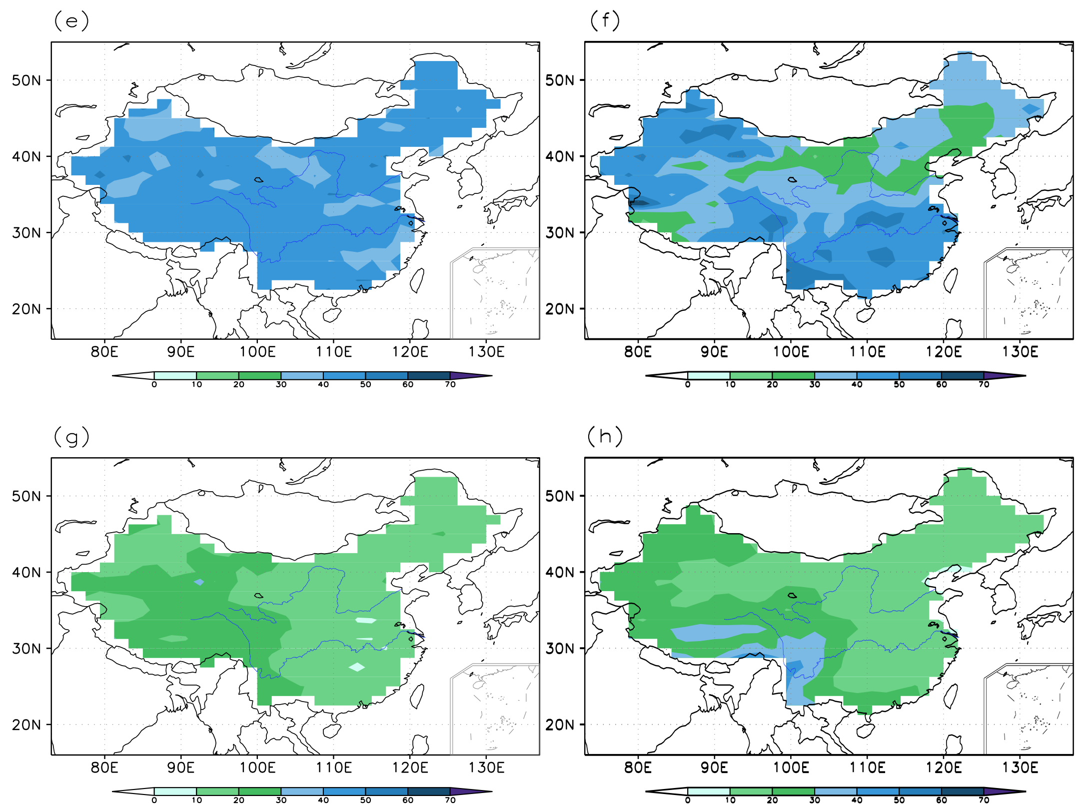

Fig. 1.(a,b)Summer (June, July, August) seasonal mean precipitation (mm day^{-1}) in the observations and model simulations for the present day (1994–2011).(c, d) Percentage contribution of heavy,(e, f) moderate and (g, h) light rainfall to the seasonal mean precipitation in the observations and models simulations.

To show the temporal and decadal variation in summer precipitation, we defined summer precipitation indexes for northern (105°E–120°E,35°N–45°N) and southern (105°E–120°E,20°N–35°N) China as the same two regions reported by Tian et al. (2018).Fig.2a shows the station distribution in China. The total summer precipitation over southern China was about548.6 mm during the early period and increased to 612.4 mm during the present day period (Fig.2b). The decadal increase in the total summer precipitation over southern China is a result of contributions from increases in both heavy and moderate precipitation, whereas there is a decrease in the contribution from light precipitation. The total summer precipitation over northern China (Fig. 2c) in the early period is about 268.2 mm, which reduces to 254.1 mm during the present day period. The decadal decrease in precipitation in north China is mainly a result of the decrease in light rainfall;

the change in moderate and heavy rainfall is not significant in this area (Fig. 2c).

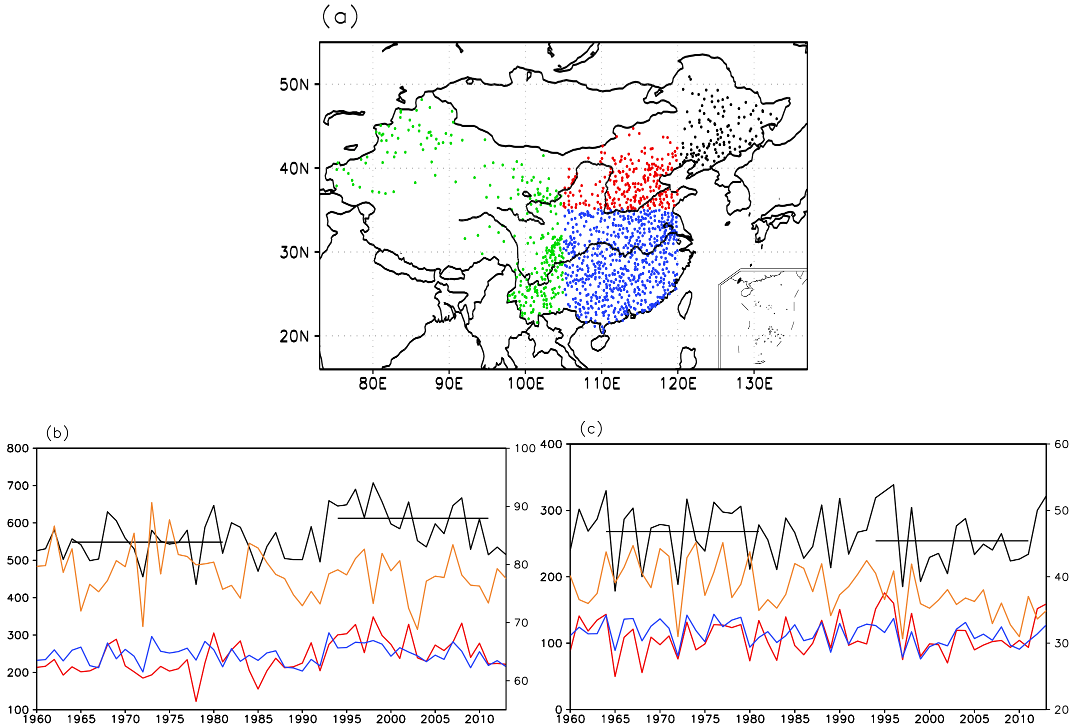

Fig.2. (a) Distribution of stations in the observational dataset. The green, red, black and blue dots represent the sub-regions of western, northern, northeastern and southern China, respectively. Time series of the area-averaged total summer precipitation (mm) based on observations over southern (b) and northern China (c), respectively. The black line is total rainfall (left-hand*y*-axis), the red line is heavy rainfall (left-hand*y*-axis), the blue line is moderate rainfall (left-hand*y*-axis) and the orange line is light rainfall (right-hand*y*-axis). The two black horizontal bars indicate the present day (1994–2011) and early period (1964–1981) rainfall.

Fig.3 shows the spatial distribution of the decadal changes in total summer precipitation, the number of dry days and the contribution of heavy, moderate and light rainfall in China across the mid-1990s in the observational dataset. Precipitation increased in southern China and decreased in northern China. This pattern is named as SFND pattern across the mid- 1990s (Fig.3a).The spatial distribution of the number of dry days shows that northern and southwestern China show opposite changes, whereas southern China show a downward trend, indicating that the change in the number of dry days contributes to the change in the total summer precipitation in the mid-1990s (Fig.3b).

According to the spatial distribution of the decadal variations in the three types of precipitation, heavy rainfall in China increases except some regions of northern and western China, and heavy rainfall in southern China increases greatly, similar to the spatial distribution of the total precipitation (Fig.3c). The changes in moderate rainfall show a decrease in most of China, with a weak increase over the mid- to lower reaches of the Yangtze River, the eastern part of southern China (south of 25° N and east of 108° E), the southern flank of the Tibetan Plateau and the western part of Xinjiang Province (Fig.3d). A significant decrease in light rainfall is seen in most of China, especially in northeastern China and the region between the Yangtze River and Yellow River (Fig.3e).These results show that the decadal increase in summer precipitation over southern China is caused by the increase in heavy and moderate rainfall, whereas the decadal decrease in precipitation over northern China in the mid-1990s is caused by the decrease in moderate and light rainfall.

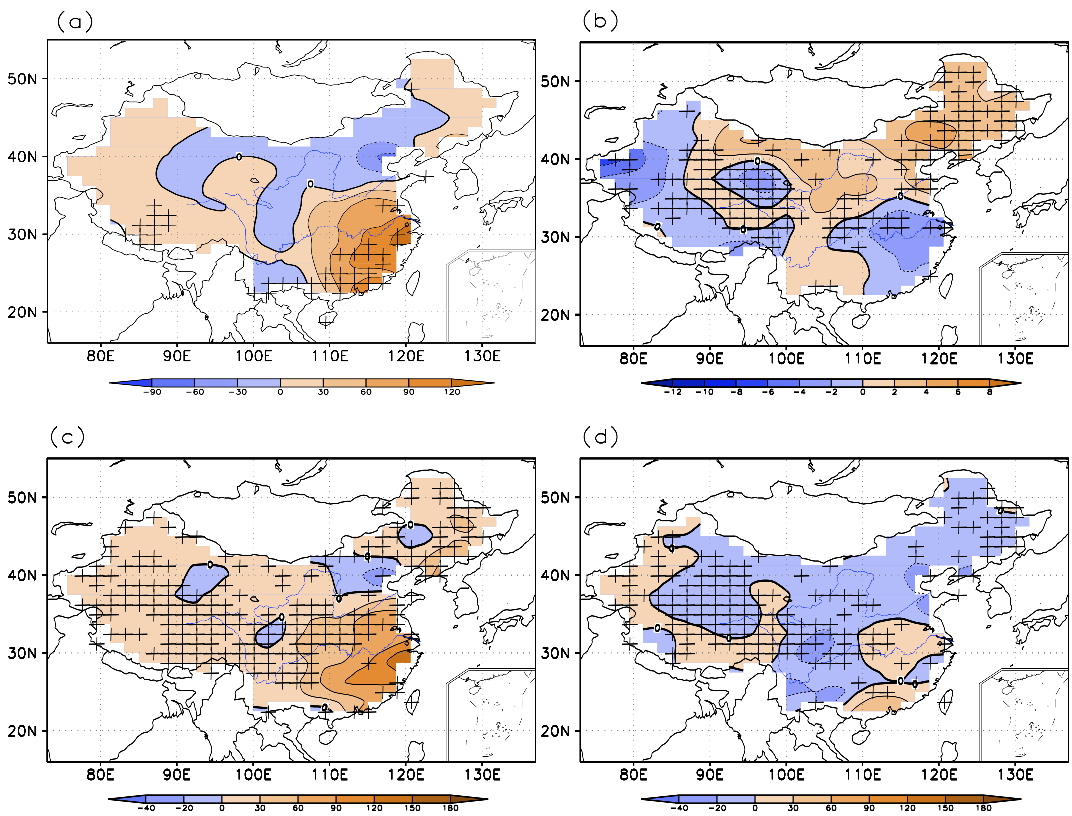

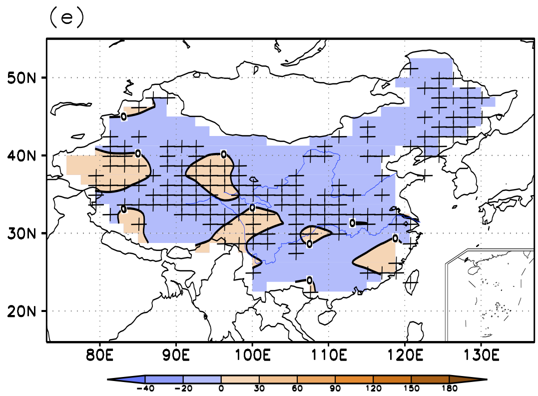

Fig.3. Spatial patterns of the differences in precipitation between the present day (1994–2011) and the early period (1964–1981) in summer. (a) Total precipitation (mm), (b) number of dry days (days) and contribution (mm) of (c) heavy, (d)moderate and (e)light rainfall in the observational dataset. The grid highlight regions where the differences are statistically significant at the 90% level using a two-tailed Student t-test.

Fig.4 shows the spatial pattern of the decadal variations in the frequency and intensity of three types of precipitation over China in the mid-1990s in the observational dataset. The main characteristics are that the frequency of heavy rainfall increases and the frequency of light rainfall decreases over most of China (Fig. 4a and 4e). The frequency of moderate rainfall increases in southern China, the western part of Xinjiang province and most part of Tibetan Plateau, whereas it decreases in northern, northeastern China, and the region between 100°E and 110°E (Fig. 4c).The intensity of heavy rainfall increases in the southern part of southern China and the eastern part of Yellow-Huai River and northeastern China, and decreases in most other areas (Fig. 4b). The intensity of moderate rainfall shows little change except in the central part of eastern China (Fig. 4d). The variation in the intensity of light rainfall in China is very weak (Fig. 4f).

These results show that the frequency and intensity of the three types of precipitation vary in different regions of China. The similarity between the frequency distribution of the three types of precipitation and the contribution of different kinds of precipitation to summer precipitation shows that the changes in frequency of the three types of precipitation dominate the overall change in summer precipitation. The frequency increase of heavy and moderate rainfall over southern China is mainly due to the increase of total rainfall. By contrast, the main reason for the decrease of summer rainfall over northern China is the decrease in the frequency of moderate and light rainfall.

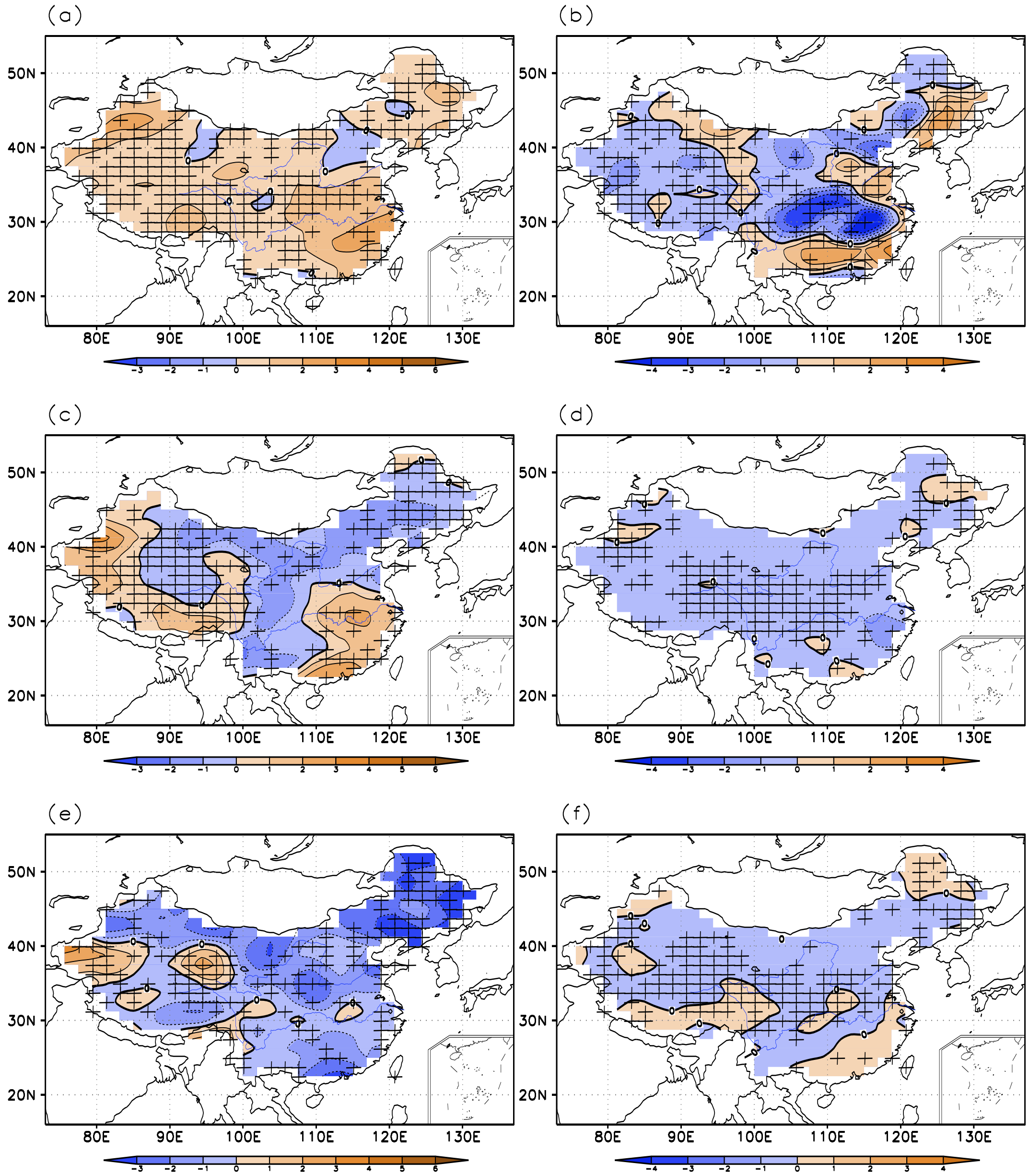

Fig.4.Spatial patterns of the differences in summer precipitation between the present day (1994–2011) and the early period (1964–1981) in the observational dataset. Frequency (number of days) of (a) heavy, (c) moderate and (e) light rainfall and intensity (mm day^{-1}) of (b) heavy, (d) moderate and (f) light rainfall. The grid highlight regions where the differences are statistically significant at the 90% level using a two-tailed Student t-test.

These observational analyses show the changes in the three types of precipitation over China with respect to their frequency, intensity and their contributions to the change in the summer seasonal mean precipitation over different regions of China across the mid-1990s. The increasing frequency of heavy and moderate rainfall is the main reasons for the increase of precipitation over southern China. The main reason for the decrease of precipitation in northern China is the decrease of the frequency of moderate and light rainfall. We carried out a series of numerical experiments to solve this question to determine the driving factors for these decadal changes in precipitation over China.

3 Model, experimental design and model climatology

3.1 Model and experiment design

The atmospheric–ocean mixed-layer coupled model MetUM-GOM1 (Hirons et al. 2015) was used to assess the contribution of changes in GHG emissions and anthropogenic aerosols together or individually to the decadal variations in precipitation in China through a set of numerical experiments. MetUM-GOML1 is a near-globally-coupled atmosphere-ocean-mixed-layer model. The coupled model comprise the Met Office Unified Model (MetUM) Global Atmosphere, version 3 (Hewitt et al. 2011; Walters et al. 2011) coupled to the Multi-Column K-profile parameterization (MC-KPP) mixed layer ocean model. The resolution in current study is 1.875° longitude and 1.25° latitude with 85 vertical layers, the model lid is at 850 km. Details about the MetUM-GOML1model and the numerical experiments (Table 1) have been reported previously by Su and Dong (2019). Firstly, we perform a relaxation experiment (R0) for 12 years, in which the present day (PD,1994-2011) greenhouses gases (GHG) and anthropogenic aerosols (AA) forcings are used and the ocean temperature and salinity were relaxed to a PD climatology, which is derived from the Met Office ocean analysis (Smith and Murphy 2007). Using different forcings, four other time-sliced experiments are performed, that is, the C-EP experiment conducted using mean GHG concentrations and AA emissions from 1964 to 1981 (EP), the C-PD-GHG experiment forced by the mean GHG concentrations during the period from 1994 to 2011 (PD), the appropriate EP mean AA emissions, and the C-PD-AA experiment forced by the PD mean AA emissions, the EP mean GHG concentrations. All experiments are run for 50 years and use the climatological PD sea ice extent from HadISST (Rayner et al. 2003). The last 45 years of each experiment are used for analysis. The same set of experiments were used to study the forcing changes of summer precipitation in East Asiaby Tian et al. (2018), the decadal changes in temperature extremes over China by Chen and Dong (2018) and the decadal changes in heatwaves by Su and Dong (2019). We used the same model and numerical experiments to study the decadal changes in precipitation over China.

Table 1 Summary of numerical experiments. Abbreviations: AA, anthropogenic aerosols; EP, early period; GHG, greenhouse gas; PD, present day.

Abbreviation	**Experiment**	**Ocean**	**Radiative forcing**
R0	Relaxation run	Relax to PD mean 3D ocean temperature and salinity to diagnose climatological temperature and salinity tendencies	Relax to PD greenhouse gases over PD and anthropogenic aerosol emissions over 1994–2010 with GHG and AA after 2006 from RCP4.5 scenario
CEP	Early period	Climatological temperature and salinity flux tendencies from relaxation run	EP mean GHG and EP mean AA emissions
CPD	Present day with GHG and AA forcing		PD mean GHG and PD mean AA emissions
CPDGHG	Present day with GHG forcing		PD mean GHG and EP mean AA emissions
CPDAA	Present day with AA forcing		EP mean GHG and PD mean AA emissions

The heavy, moderate and light rainfall in the experiments were defined in the same way as in the observational dataset and the relative thresholds were calculated as the daily 90th and 60th percentiles of precipitation based on the last 45 years of the CEP experiment. A pair of experiments contains and excludes a specific forcings, and the difference between the two experiments represents the response to the compulsion. The difference between the CPD and CEP experiments shows the combined influence of changes in both GHG concentrations and the emission of anthropogenic aerosols (hereafter referred to as ALL forcing). The influence of greenhouse gas concentration change (hereinafter referred to as GHG forcing) is the difference between cpdghg and CEP models, while the impact of anthropogenic aerosol emission change (hereinafter referred to as AA forcing) is the difference between cpdaa and CEP models.

3.2 Model climatology

Fig.1(b,d,f,h) shows the simulated summer precipitation and the contributions of the three types of precipitation to the summer seasonal mean values in the present day simulation. The main feature of the summer precipitation simulated by the model is that there is more precipitation over southern China and less precipitation over northwestern China (Fig. 1b), with heavy rainfall accounting for 30–40% of summer precipitation over large areas of eastern China and accounting for about 10–30% of summer precipitation over western China (Fig. 1d). Moderate rainfall explains about 50–60% of summer precipitation. This contribution is about 10% higher than in the observational dataset and 10% higher than the contribution from heavy precipitation in the model simulation (Fig. 1c, 1d, 1e and 1f). The contribution from light precipitation shows the form of west more and east less that accounts for<20% of summer precipitation in eastern China and 20–30% over western China, which is similar to the observational dataset. These results show that the main characteristics of summer precipitation and the contributions of the three types of precipitation to summer precipitation in the observational dataset are well reproduced by the MetUM-GOML1 model.

4 Model simulated responses to different anthropogenic forcings

4.1 Spatial pattern of responses to different forcings

Fig. 5 shows the spatial patterns of changes in the total summer precipitation in response to ALL forcing and GHG forcing and AA forcing. By ALL forcing, the total precipitation shows a + − + pattern from north to south over China east of 100° E. Precipitation increases over southern and northeastern China, but decreases over northern and most parts of southwestern and northwestern China which is similar to the variability of precipitation calculated by the observational dataset. Through comparison, it is found that the increase of precipitation in southern China and northeastern China is mainly caused by greenhouses gases emissions, while the decrease of precipitation in northern China and most parts of southwestern and northwestern China is mainly caused by anthropogenic aerosols.

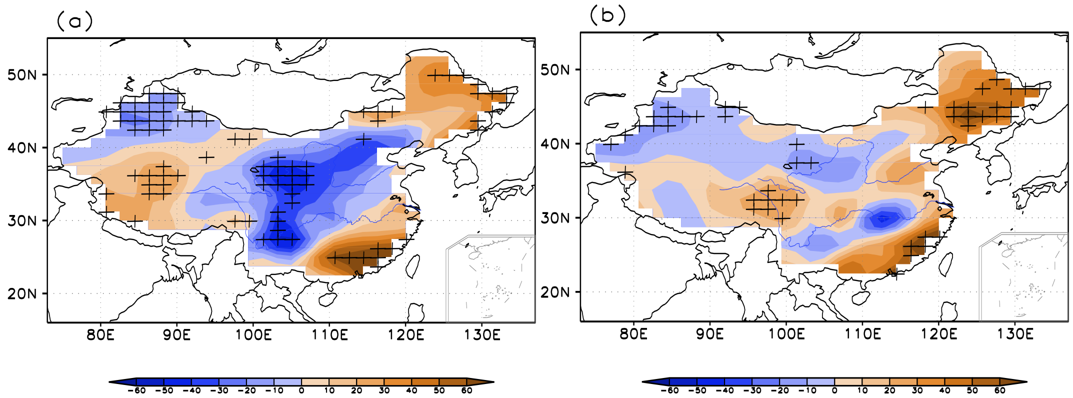

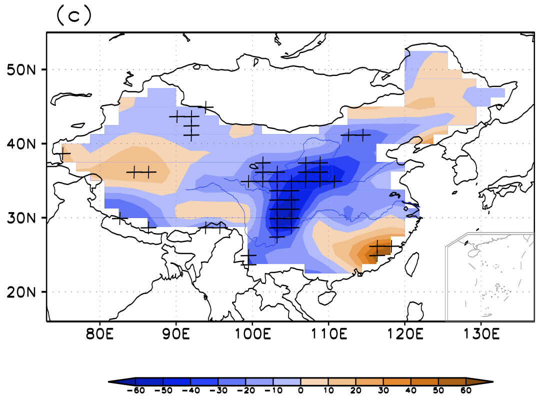

Fig.5 The changes of the total summer precipitation in response to ALL forcing (a) and GHG forcing (b) and AA forcing (c). The grid highlight regions where the differences are statistically significant at the 90% level using a two-tailed Student t-test.

Fig.6 shows the spatial patterns of changes in the contributions from heavy, moderate and light rainfall in response to ALL forcing. The increase in heavy rainfall is the main reason for the increase in summer total precipitation in southern China in the ALL forcing experiment (Fig.6a), which is consistent with the observational dataset(Fig. 3c). However, the region in which precipitation and the contribution of heavy rainfall increase simulated by the model is located over southeastern China and there is no clear northward expansion. The decrease in heavy, moderate and light rainfall over northern China leads to the decrease in the total summer precipitation, consistent with the observational dataset.

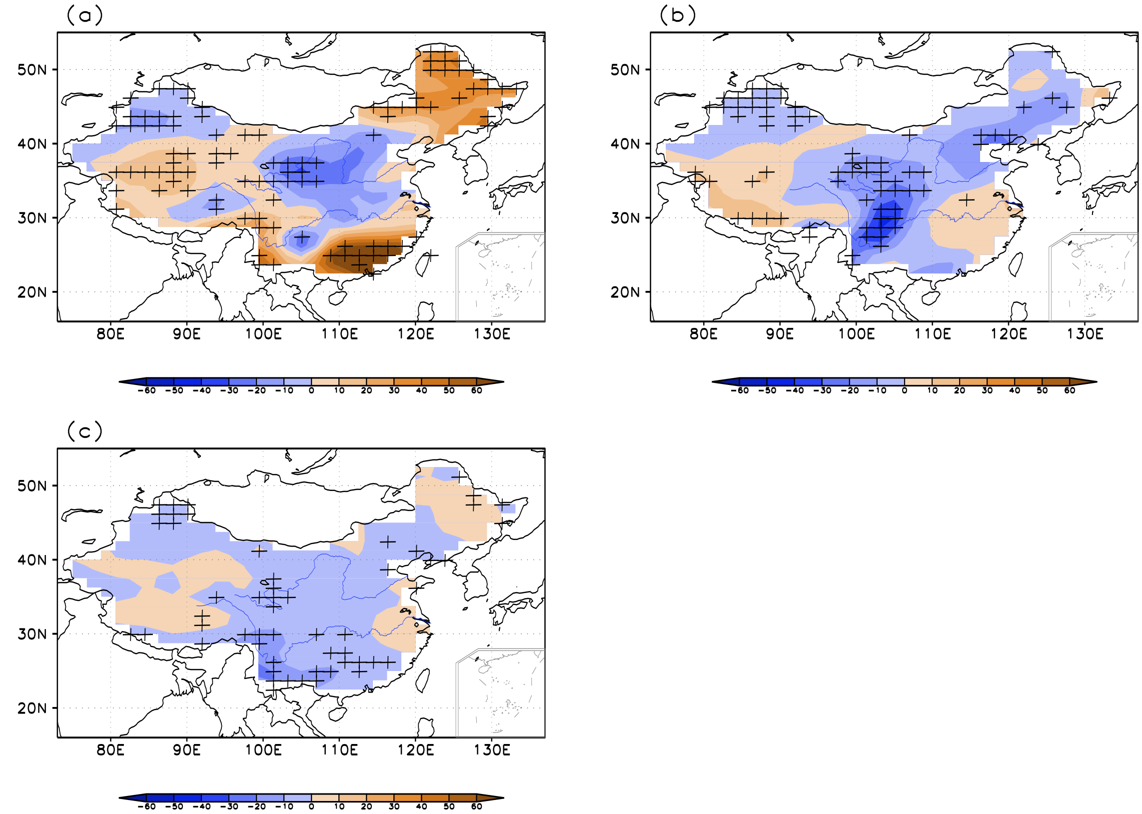

Fig.6.Model simulated changes in (a) heavy rainfall, (b) moderate rainfall and (c) light rainfall (mm) in response to ALL forcing (CPD-CEP). The grid highlight regions where the differences are statistically significant at the 90% level using a two-tailed Student t-test.

Because the variation in heavy rainfall is the main contributor to the change in total precipitation in summer, Fig.7 shows the changes in the frequency and intensity of heavy rainfall in the ALL forcing experiment. In the ALL forcing experiment, the principle features of the changes in heavy precipitation are that the frequency increases significantly over southern and northeastern China, and most of the area west of 100°E, but decreases over northern China (Fig.7a). These main features have some spatial similarities with the observed changes (Fig. 4a), although the spatial extent of the decrease in frequency of heavy rainfall over northern China is larger than in the observational dataset. The change of intensity in heavy precipitation in response to changes in ALL forcing (Fig.7b) show an+ − +pattern from northern China to southern China, is consistent with the observational datasets (Fig. 4b). These changes are more similar to the spatial variations in the changes in frequency than in the changes in intensity, indicating a dominant role of the changes in frequency, consistent with the observational dataset.

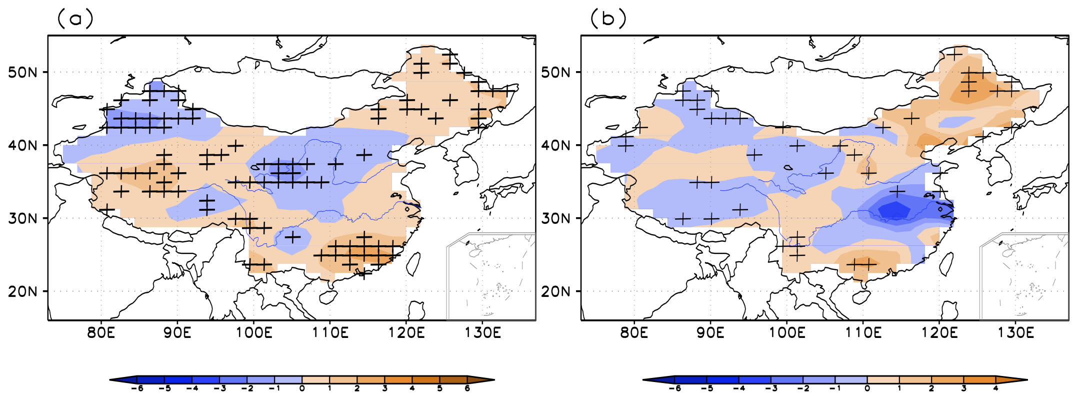

Fig.7.Model simulated changes in (a) frequency (number of days) and (b) intensity (mm day^{-1}) of heavy rainfall in response to changes in ALL forcing. The grid highlight regions where the differences are statistically significant at the 90% level using a two-tailed Student t-test.

Separate forcing experiments suggested that changes in the concentration of GHG emissions increase the frequency of heavy rainfall over almost all regions of China, especially over southern and northeastern China, whereas changes in anthropogenic aerosols play a dominant part in reducing the frequency of heavy rainfall over northern China (Fig. 8a and 8b). The variation in intensity of heavy rainfall in response to GHG forcing (Fig.8c) is similar to that in the ALL forcing experiment (Fig.7b), especially the increased intensity over the eastern part of northern and northeastern China and the decreased intensity over southern China. The results indicate that the dominant contribution of anthropogenic changes to changes in summer precipitation is mainly realized by the changes in the frequency of heavy rainfall. The increase in the concentration of GHGs plays an important part in the increase in summer precipitation over southern China and northeastern China, which is mainly caused by the increase in the frequency of heavy rainfall. The changes in anthropogenic aerosols are important in the decrease in precipitation over northern China, which is mainly due to the decrease in the frequency of heavy rainfall (Fig. 8).

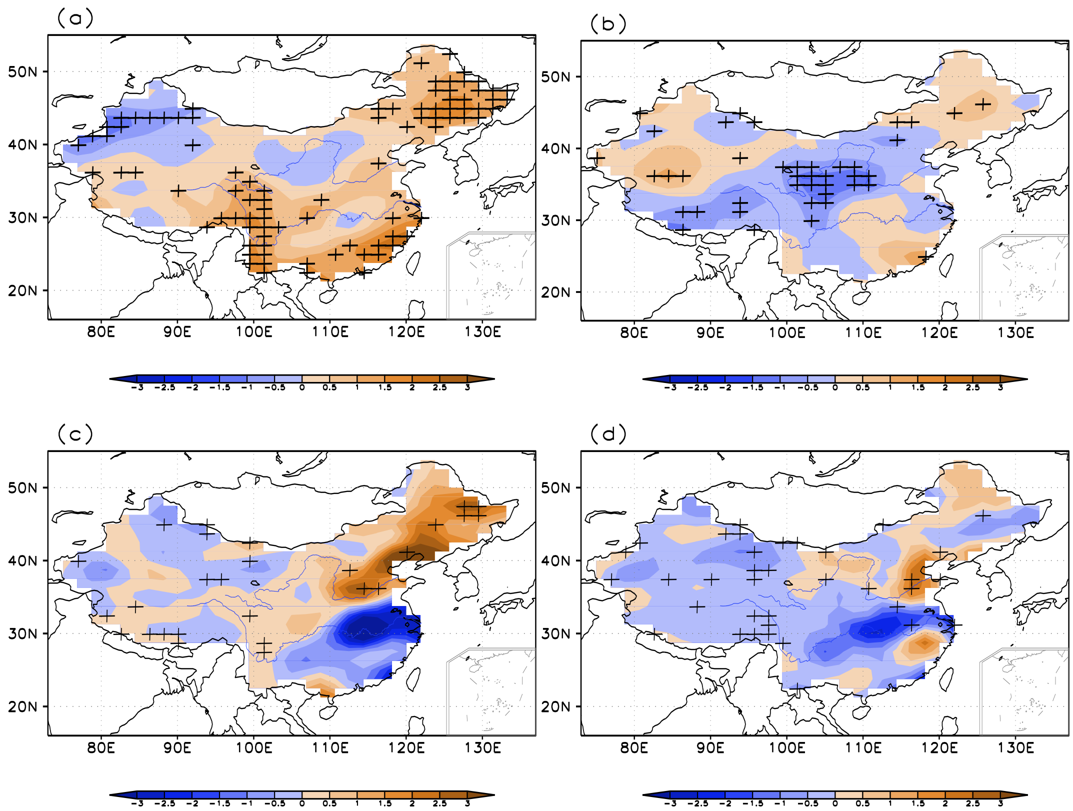

Fig.8.Model simulated changes in frequency (number of days) of heavy rainfall in response to changes in (a) GHG forcing and (b) anthropogenic aerosol forcing. Model simulated changes in intensity (mm day^{-1}) of heavy rainfall in response to changes in (c) GHG forcing and (d) anthropogenic aerosol forcing. The grid highlight regions where the differences are statistically significant at the 90% level using a two-tailed Student t-test.

4.2 Area-averaged responses to different forcings

Based on the unique characteristics of the climate in China, we studied the decadal changes in precipitation in four sub-regions of China: northern China (105°E–120°E,35°N–45°N), northeastern China (north of 40°E and east of 120°E), southern China (105°E–120°E, 20°N–35°N) and western China (west of 105°E). Fig.2a shows the distribution of the stations over the four sub-regions. Fig.9 shows the area-averaged changes in the frequency of the three types of precipitation over the four sub-regions for both the observational dataset and the model experiments. Besides the change in frequency of heavy rainfall in northern China, moderate rainfall in southern China and light rainfall in northeastern China, the changes in the three types of precipitation in response to the changes in ALL forcing simulated by the model are consistent with the observational dataset. The simulated increases in the frequency of heavy precipitation by ALL forcing averaged over southern, northeastern and western China are similar to the observed changes, but the increases in frequency over southern and western China are weaker than the observed changes (Fig. 9a). Changes in GHG emissions play a leading part in the changes in frequency averaged over southern, northeastern and western China. The changes in the frequency of moderate rainfall averaged over northern, northeastern and western China in the ALL forcing experiment are close to those in the observations (Fig. 9b). Changes in anthropogenic aerosols play a key part in the changes in the frequency of moderate rainfall over northern and northeastern China. The simulated changes in the frequency of light rainfall averaged over northern, southern and western China in the ALL forcing experiment are close to those in the observational dataset (Fig. 9c).The variations in light rainfall over southern, northern and western China are clearly influenced by the changes in GHG emissions.

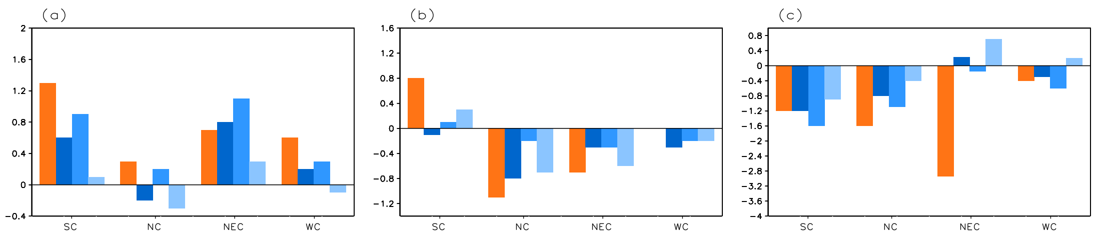

Fig.9. Area-averaged changes in frequency (number of days) of (a) heavy rainfall, (b) moderate rainfall and (c) light rainfall (mm day^{-1})over southern, northern, northeastern and western China in the observational dataset (orange bars) and the simulations forced by ALL forcing (dark blue bars), GHG forcing (blue bars) and anthropogenic aerosol forcing (light blue bars).

Fig.10 shows the area-averaged changes in intensity of the three types of precipitation over the four sub-regions for both the observational dataset and the model experiments. For heavy rainfall, as presented by Fig.10a, the observed decreases in the intensity of precipitation averaged over southern China are simulated by the ALL forcing, but the change is underestimated. The changes in the concentration of GHGs explain the response in the simulated changes of heavy precipitation over southern and northeastern China, indicating the predominant role of changes in GHG emissions in influencing the intensity of heavy rainfall. For moderate rainfall, the changes in intensity averaged over northern, southern and western China in the ALL forcing experiment are close to those in the observational dataset (Fig. 10b). Changes in anthropogenic aerosols play a key part in causing the changes in the intensity of moderate rainfall over southern, northern and western China. For light rainfall, the simulated changes in intensity averaged over western China in the ALL forcing experiment are close to those in the observational dataset, although the simulated changes in intensity over western China are clearly overestimated. The changes in light rainfall over western China are significantly influenced by the changes in GHG concentrations, indicating the predominant role of GHG emissions in affecting the intensity of light rainfall (Fig. 10c).

The simulated changes in the frequency of different types of precipitation are more consistent with those in the observational dataset than the simulated changes in intensity. The model simulations also show that changes in the frequency of different types of precipitation affect the contribution of the different types of precipitation to the changes in the total summer precipitation, in agreement with the observational database.

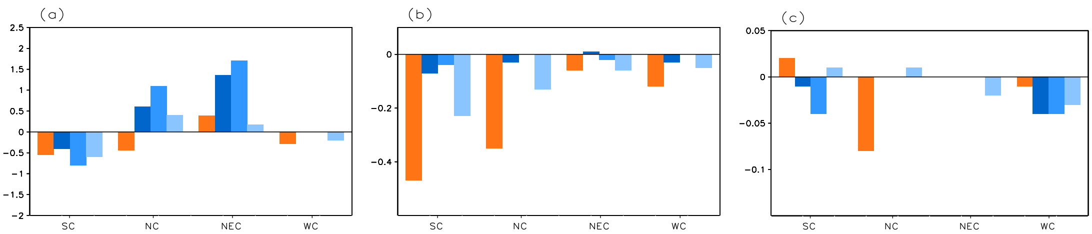

Fig.10. Area-averaged changes in intensity (mm day^{-1}) of (a) heavy rainfall, (b) moderate rainfall and (c) light rainfall over southern, northern, northeastern and western China in the observational database (orange bars) and simulations forced by ALL forcing (dark blue bars), GHG forcing (blue bars) and anthropogenic aerosol forcing (light blue bars).

5. Physical processes responsible for the simulated decadal changes of precipitation

Firstly, we present the difference of the 850-hPa water vapor flux divergence and water vapor flux between CPD and CEP experiments in summer by the different forcing. During summer, the water vapor flux convergence in response to ALL forcing appears most area to the east of 110°E and to the south of the Yangtze River and northeastern China. The warm and southwesterly flow transports moist to the above two regions and it is beneficial to the occurrence of precipitation in the above two areas. Over northern and southwestern China, water vapor flux divergence and the implicit water vapor flux transport are not conductive to the occurrence of precipitation (Fig.11a). From the pattern by GHG forcing, we can see that the water vapor flux convergence appear in southern China and northeastern China. The water vapor flux in the above regions is significantly higher than that in ALL forcing. This distribution is also conductive to precipitation in southern China and northeastern China (Fig.11b). As far as the result of AA forcing is concerned (Fig.11c), the obvious water vapor flux convergence appear the southeastern China only and the southwesterly water vapor transport is also significantly weakened. In addition, the weak water vapor flux divergence is located in southwestern China, eastern part of northern China and Yellow-Huai River. Under the control of weaken southwesterly winds and 850-hPa divergence, precipitation decreases over northern and southwestern China (Fig.5c).

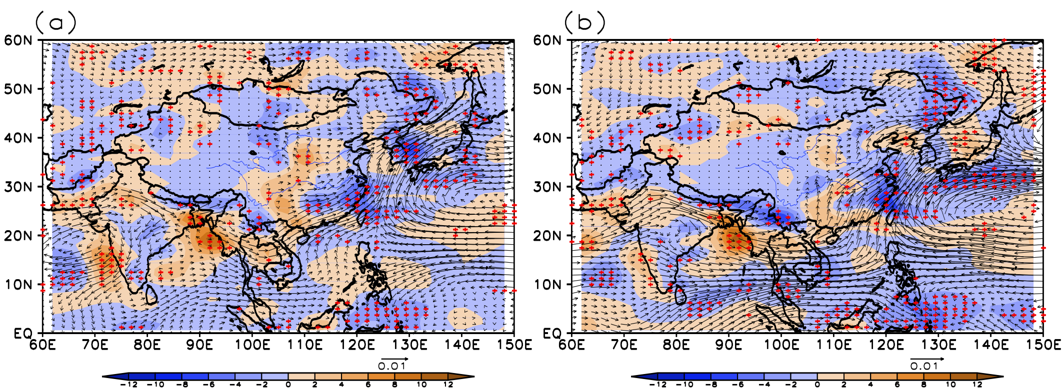

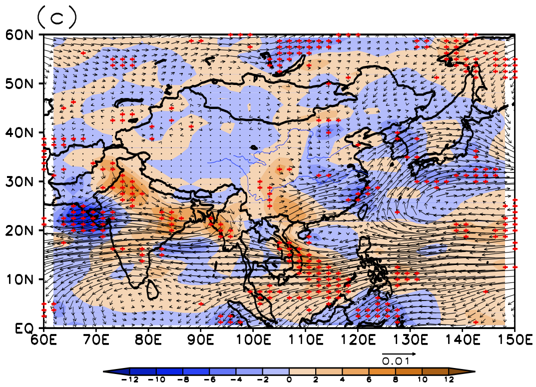

Fig.11 The difference of 850-hPa water vapor flux divergence and water vapor flux between PD and EP experiments in JJA in response to ALL forcing (a), GHG forcing (b) and anthropogenic aerosol forcing (C). The grid highlight regions where the differences are statistically significant at the 90% level using a two-tailed Student t-test.

Fig.12 show the difference of the vertical velocity and air temperature between CPD and CEP experiments in JJA in response to ALL forcing, GHG forcing and AA forcing In response to ALL forcing (Fig.12a), the air temperature warms over troposphere between 0-50°N, corresponding to ascent between 20°N-30°N and descent between 30°N-40°N. In response to GHG forcing (Fig.12b), the rise of the air temperature between 0-40°N is especially evident. The ascending movement decreases between 20°N-30°N and increases between 30°N-40°N. In response to AA forcing (Fig.12c), the tropospheric temperature decreases obviously, and the pattern of vertical velocity is similar to that by ALL forcing.

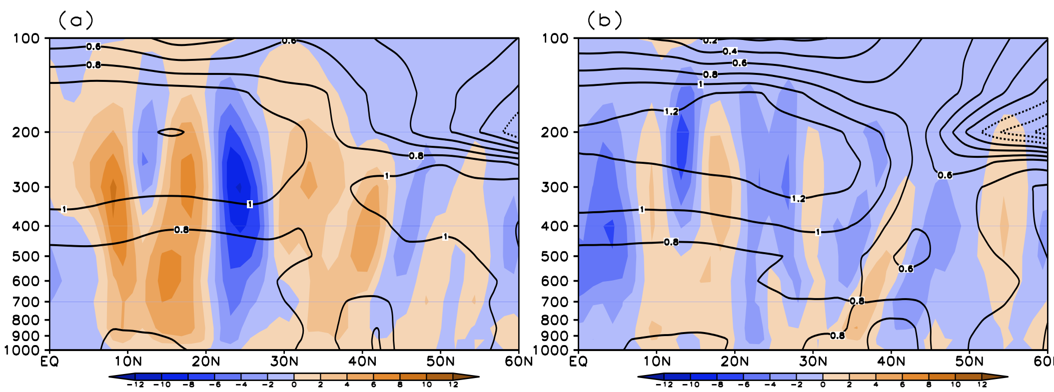

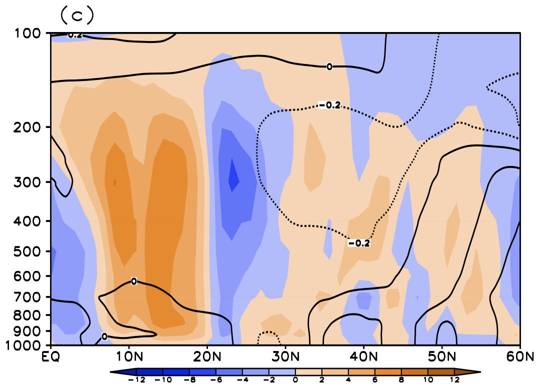

Fig.12 Vertical velocity and surface air temperature difference between PD and EP experiments in JJA in response to ALL forcing (a), GHG forcing (b) and anthropogenic aerosol forcing (C).

6. Conclusions

We determined the decadal changes in the frequency and intensity of three types of summer precipitation (heavy, moderate and light rainfall) across the mid-1990s based on an observational dataset. A set of numerical time-slice experiments was carried out using an atmosphere–ocean mixed-layer coupled model to assess the impact of human activities, includingchanges in GHG concentrations and anthropogenic aerosols emissions, in the decadal changes of heavy rainfall. Our main conclusions are follows.

The analyses of the observed precipitation show increases over southern China, but decreases over northern and southwestern China from the early period of 1964–1981 to the present day period of 1994–2011.The decadal increase in summer precipitation over southern China is caused by the increase in heavy and moderate rainfall, whereas the decadal decrease in precipitation over northern China in the mid-1990s is caused by the decrease in moderate and light rainfall. The main reason for the decrease in summer precipitation over northern China is the decrease in the frequency of moderate and light rainfall. The increases in frequency of heavy and moderate rainfall over southern China are the main causes of the increases in total precipitation.

Numerical model experiments show that the changes in anthropogenic aerosol emissions have a dominant role in the frequency of heavy rainfall over northern China and that the response to GHG forcing is more significant for the frequency of heavy precipitation over southern and northeastern China. The increase of precipitation frequency forced by greenhouses gases is the main reason of increasing precipitation over southern and northeastern China, while the decrease of frequency caused by anthropogenic aerosols induces the decreasing precipitation over northern China.

By the analysis of preliminary physical mechanism, we found that the water vapor flux convergence strengthens in southern and northeastern China by GHG forcing, and the water vapor flux in the above regions enhances too. This distribution is also conductive to precipitation in southern and northeastern China. From the atmospheric circulation of AA forcing we can find that the obvious water vapor flux convergence appears over southeastern China only and the southwesterly water vapor transport is also significantly weakened. In addition, the weak water vapor flux divergence is located in southwestern China, eastern part of northern China and Yellow-Huai River. Under the control of weaken southwesterly winds and 850-hPa divergence, precipitation decreases over northern and southwestern China.

This paper mainly studies the individual roles of GHG concentrations and AA emissions in the decadal changes of the three types of summer precipitation over China. Based on the change of total precipitation, a preliminary physical mechanism analysis is given, and the causes of change of precipitation frequency and intensity need further study in the future.

Acknowledgments

This work was jointly sponsored by the National Science Foundation of China (Grant 41905091), the Support Plan of the National Science and Technology (2015BAC03B04) and the

Fund project of the National Meteorological Center Forecaster (Grant Y201904) BD is supported by the UK National Centre for Atmospheric Science–Climate (NCAS-Climate) at the University of Reading.

Reference

Arribas A, Glover M, Maidens A, et al., 2011:The GloSea4 ensemble prediction system for seasonal forecasting.*Mon.Wea.Rev.,*139,1891-1910,doi: 10.1175/2010MWR3615.1

Bollasina MA, Ming Y, Ramaswamy V., 2011: Anthropogenic aerosols and the weakening of the South Asian summer monsoon. Science 334,502-505,doi: 10.1126/science.1204994

Caesar J, Lowe JA.,2012: Comparing the impacts of mitigation versus non-intervention scenarios on future temperature and precipitation extremes in the HadGEM2 climate model.*Geophys. Res. Lett.,*117,D15109,doi:10.1029/2012JD017762

Chen, H., J. Sun,2017: Anthropogenic warming has caused hot droughts more frequently in China. *J. Hydrol.,*544,306-318,doi:10.1016/j.jhydrol.2016.11.044

Chen,W., B. W. Dong,2018: Anthropogenic impacts on recent decadal change in temperature extremes over China: relative roles of greenhouse gases and anthropogenic aerosols. *Climate Dyn.*,doi:10.1007/s00382-018-4342-9.

Ding, Y.H., Z. Y. Wang, Y. Sun,2008: Intern-decadal variation of the summer precipitation in East China and its association with decreasing Asian summer monsoon. Part i: observed evidences. Int.*J. Climatol.*, 28,1139-1161,doi:10.1002/joc.1615.

Ding Y.H., Y. Sun, Z. Y. Wang, et al.,2009: Inter-decadal variation of the summer precipitation in China and its association with decreasing Asian summer monsoon PartⅡ:possible causes. Int.*J.*

Climatol.,29,1926-1944,doi:10.1002/joc.1759.

Dong B, Sutton RT, Highwood EJ, et al.,2016:Preferred response of the East Asian summer monsoon to local and non-local anthropogenic sulphur dioxide emissions. *Climate Dyn.*,46,1733-1751,doi:10.1007/s00382-015-2671-5.

Dong B, Sutton RT, Shaffrey L, et al.,2017:Attribution of forced decadal climate change in coupled and uncoupled ocean-atmosphere model experiments. *J.Clim.*, 30, 6203-6223,doi:1-.1775/JCLI-D-16-0578.1.

Fan, K., Z.Q.Xu, B.Q.Tian, 2014: Has the intensity of the interannualvariability in summer rainffall over South China remarkably increased? *Meteor.Atmos. Phys.,*124,23-32,doi:10.1007/s00703-013-0301-5.

Gong D.Y., Ho CH., 2002:Shift in the summer rainfall over the Yangtze River valley in the late 1970s. *Geophys. Res. Lett.*,doi:10.1029/2001GL014523

Hirons, L. C., Klingaman, N. P., Woolnough, S. J., 2015:MetUM-GOML: a near-globally coupledatmosphere-ocean-mixed-layer model. *Geosci Model Dev.,*8, 363-379,doi:10.5194/gmd-8-363-2015.

He B.R., P.M.Zhai, 2018:Changes in persistent and non-persistent extreme precipitationin China from 1961 to 2016. *Advances in Climate Change Research,*9,177-184,doi:10.1016/j.accre.2018.08.002.

Kharin VV, Zwiers F, Zhang X, et al., 2013:Changes in temperature and precipitation extremes in the CMIP5 ensemble. *Clim.Change,*119,345-357,doi:10.1007/s10584-013-0705-8

Lamarque JF, Bond TC, Eyring V, et al.,2010: Historical (1850-2000) gridded anthropogenic and biomass burning emissions of reactive gases and aerosols: methodology and application. *Atmos.*

Chem. Phys., 10,7017-7039,doi:10.5194/acp-10-7017-201

Lamarque JF, Kyle GP, Meinshausen M, et al., 2011:Global and regional evolution of short-lived radiatively-active gases and aerosols in the representative concentration pathways.*Clim.Change,*109 ,191,doi:10.1007/s10584-011-0155-0.

Liu, R., S.C.Liu, R. J. Cicerone, et al., 2015: Trends of extreme precipitation in Eastern China and their possible causes.*Adv. Atmos. Sci.,* 32,1027-1037,doi:10.1007/s00376-015-5002-1

Min,S., Y.F.Qian,2008:Regionality and persistence of extreme precipitation events in China. *Adv. Water. Sci.,* 19,763-771,doi:10.3724/SP.J.1047.2008.00014

Ma S.M., T.J.Zhou, Stone DA, et al., 2017b: Detectable anthropogenic shift toward heavy precipitation over eastern China.*J.Clim.,*30,1381-1396,doi:10.1175/jcli-d-16-0311.1.

Pendergrass,A., D.L.Hartmann,2014a:The atmospheric energy constraint on global-mean precipitation change. *J.Clim.,*27,757-768,doi:10.1175/JCLI-D-13-00163.1.

Qian, W.H., Qin.,2008: Precipitation division and climate shift in China from 1960 to 2000. *Theor. Appl. Climatol.,* 93, 1-17,doi:10.1007/s00704-007-0330-4

Qian,Y.,D.Y.Gong, J.W.Fan, et al., 2009:Heavy pollution suppresses light rain in China: Observations andmodeling.*J.Geophys.Res. Atmos.,* 114,D00K02,doi:10.1029/2008JD011575.

Rajah,K.,T.O'Leary, A. Turner, et al.,2014:Changes to the temporal distribution of daily precipitation, *Geophys. Res. Lett.*,41,8887-8894,doi:10.1002/2014GL062156.

Rayner NA, Parker DE, Horton EB, et al.,2003: Global analyses of sea surface temperature, sea ice, and night marine air temperature since the late nineteenth century. *J.Geophys.Res.Atmos.,*108,1-37,doi:10.1029/2002jd002670

Ren Z., Y. Yu, F.L.Zou, et al.,2012: Quality detection of surface historical basic meteorological data.

J. Appl Meteor Sci, 23: 739-747,doi:10.1007/s11783-011-0280-z

Rosenfeld,D.,J.Dai,X.Yu,et al., 2007: Inverse relations between amounts of air pollution and orographic precipitation. Science, 315,1396-1398,doi:10.1126/science.1137949

Shen C., W.C.Wang, Z.Hao, et al.,2008:Characteristics of anomalous precipitation events over eastern China during the past five centuries.*ClimateDyn.*, 31,463-476,doi:10.1007/s00382-007-0323-0

Sillmann J, Pozzoli L, Vignati E, et al.,2013a: Aerosol effect on climate extremes in Europe under different future scenarios.*Geophys. Res. Lett.*, 40,2290-2295,doi:10.1002/grl.50459

Smith DM, Murphy JM, 2007:An objective ocean temperature and salinity analysis using convariances from a global climate model.*J.Geophys.Res. Oceans*,112,1-19,doi:10.1029/2005JC003172

Song,F., T. Zhou, Y. Qian, 2014: Responses of East Asian summer monsoon to natural and anthropogenic forcings in the 17 lates CMOP5 models. *Geophys. Res. Lett.*, 41, 596-603,doi:10.1002/2013GL058705

Su, Q., B.W.Dong, , 2019: Recent decadal changes in heat waves over China: drivers and mechanisms. *J.Clim.,*32,4215-4234,doi:10.1175/JCLI-D-18-0479.1.

Tian, F.X., B.W.Dong,, John Robson, et al., 2018:Forced decadal changes in the East Asian summer monsoon: the roles of greenhouse gases and anthropogenic aerosols.*ClimateDyn.,*doi:10.1007/s00382-018-4105-7.

Trenberth,K.E.,1999:Conceptual framework for changes of extremes of the hydrological cycle with climate change. *Climatic Change*,42:327-339,doi:10.1023/A:1005488920935.

Walters DN, Best MJ, Bushell AC, et al.,2011: The met office unified model global atmosphere

3.0/3.1 and JULES global land 3.0/3.1 configurations. Geosci Model DEV 4,919,doi:10.5194/gmd-4-919-2011

Wan, H., X. B.Zhang, ,F. W. Zwiers, et al., 2015:Attributing northern high-latitude precipitation change over the period 1966-2005 to human influence. *Climate Dyn.,* 45, 1713-1726,doi:10.1007/s00382-014-2423-y

Wang, Y., Q.Wan,,W.Meng,,et al.,2011:Long-term impacts of aerosols on precipitation and lightning over the Pearl River Delta megacity area in China.*Amos. Chem. Phys.,* 11,12,421-436,doi:10.5194/acp-11-12421-2011

Wang, Y., Po-Lun Ma, Honathan H., et al.,2016: Toward reconciling the influence of atmospheric aerosols and greenhouse gases on light precipitation changes in Eastern China. *J.Geophys.Res. Atmos.,* 5878-5887,doi:10.1 002/2016JD024845.

Wang T, Oteera OH, Gao YG, et al., 2012: The response of the North Pacific Decadal Variability to strong tropical volcanic eruptions.*ClimateDyn.,* 39,2917-2936,doi:10.1007/s00382-012-1373-5

Wang, T., H.J.Wang, Ottera OH, et al., 2013: Anthropogenic agent implicated as a prime driver of shift in precipitation in eastern China in the late 1970s. *Atmos. Chem. Phys.*,13,12433,doi:10.5194/acp-13-12433-2013

Wu, R., L.Chen, ,1998:Decadal variation of summer rainfall in the Yangtze-Huaihe River valley and its relationship to atmospheric circulation anomalies over East Asian and western North Pacific. *Adv. Atmos. Sci.,* 15,510-522,doi:10.1007/s00376-998-0028-2

Wu, R.G., Z.P.Wen,,S.Yang,,et al.,2010:An interdecadal change in southern China summer rainfall around 1992/1993. *J. Clim.,*23,2389-2403,doi:10.1175/2009JCLI3336.1

Xie, X., H.Wang,, X.Liu,, et al., 2016:Distinct effects of anthropogenic aerosols on the East Asian summer monsoon between multidecadal strong and weak monsoon stages.*J.Geophys.Res.,* Atmos.121: 7026-7040,doi:10.1002/2015JD024228.

Xu, Z.Q., K.Fan,,H.J.Wang,, 2015:Decadal variation of summer precipitation over China and associated atmospheric circulation after the late 1990s. *J. Clim.,*28,4086-4106,doi:10.1175/JCLI-D-14-00464.1.

Yang, X.,Z.Q.Li,,2014:Increases in thunderstorm activity and relationships with air pollution in southeast China, *J.Geophys.Res. Atmos.,*119,1835-1844,doi:10.1002/2013JD021224

Yao. C., S. Yang, W. Qian, et al., 2008:Regional summer precipitation events in Asia and their changes in the past decades.*J.Geophys.Res.Atmos.,*113, D17107,doi:10.1029/2007JD009603.

Yu, R.C., B.Wang,,T.J.Zhou,, 2004:Tropospheric cooling and summer monsoon weakening trend over East Asia.*Geophys. Res. Lett.,*31,L22212,doi:10.1029/2004gl021270

Yu, R.C., T.J.Zhou,, 2007:Seasonality and three dimensional structure of interdecadal change in the East Asian monsoon. *J. Clim.,* 20, 5344-5355,doi:10.1175/2007JCLI1559.1

Zhai,P.M., X.B.Zhang, ,H.Wan,, et al.,2005: Trends in total precipitation and frequency of daily precipitation extremes over China. *J. Clim.,* 18,1096-1108,doi:10.1175/JCLI-3318.1.

Zhang, L.X., P.L.Wu,, T.J.Zhou,,2017: Aerosol forcing of extreme summer drought over North China. *Environ. Res.Lett.,* 12:034020,doi:10.1088/1748-9326/aa5fb3.

Zhao, P., S.Yang,,R.C.Yu,, 2010: Long-term changes in rainfall over eastern China and large-scale atmospheric circulation associated with recent global warming. *J. Clim.,* 23,1544-1562,doi:10.1175/2009JCLI2660.1.Zhou, B.T., Q.H.Wen,, Y.Xu,, et al., 2014:Projected changes in temperature and precipitation extremes in China by CMIP5 multimodel ensembles.

*J. Clim.,*27,6591-6611,doi:10.1175/JCLI-D-00761.1.

Zhou, T.J., D.Y.Gong,,J.Li,, et al.,2009:Detecting and understanding the multi-decadal variability of the East Asian summer monsoon-Recent progress and state of affairs. *Meteor. Z.*, 18,455-467,doi:10.1127/0941-2948/2009/0396